



# *Ilex paraguariensis* extracts and its polyphenols prevent oxidative damage and senescence of human retinal pigment epithelium cells

Pablo S. Tate, Mariela C. Marazita, Melisa D. Marquioni-Ramella, Angela Maria Suburo\*

Instituto de Investigaciones en Medicina Traslacional (IIMT), CONICET and Facultad de Ciencias Biomédicas, Universidad Austral, Pilar B1629AHJ, Buenos Aires, Argentina

## ABSTRACT

Aged-related macular degeneration (AMD), a prevalent chronic disease leading to blindness, is associated with oxidative damage of the retinal pigment epithelium (RPE). *Ilex paraguariensis* (yerba mate, YM), widely consumed in South America, is an excellent source of antioxidants and could prevent RPE cell impairment. Therefore, we evaluated the effects of YM extracts or caffeic (CAF) and chlorogenic (CHL) acids, two major *Ilex* polyphenols on cell death or premature senescence in a cell line derived from human RPE (ARPE-19). Cultures were incubated with YM, CAF, CHL or appropriate controls and then exposed to H<sub>2</sub>O<sub>2</sub>. Protection was correlated with decreases of reactive oxygen species (ROS) and DNA breaks, phosphorylation of the cAMP response element (CREB) and increases of the nuclear factor erythroid 2-related factor 2 (NRF2), BCL2, superoxide dismutase (SOD2) and sirtuin 1 (SIRT1). These results support the protective role of YM and its polyphenols against oxidative stress induced RPE injury.

## 1. Introduction

The retinal pigment epithelium (RPE) is a cell monolayer placed between the outer retina and the vascular choroid. RPE cells associate to photoreceptor cells, rods and cones, which transform light into electrochemical signals. The highest photoreceptor density occurs in the macula lutea, rich in xanthophyll pigments and essential for photopic, high acuity vision (Provis, Penfold, Cornish, Sandercoe, & Madigan, 2005). The outer retina is avascular and exchanges nutrients and metabolites with the choroid vessels through the RPE. The high metabolic activity and oxygen consumption, together with exposure to light, generate an oxidative environment. In addition, the huge concentration of membranous discs containing the photosensitive molecules (opsins) contribute to the accumulation of oxidized lipids in photoreceptors (Marquioni-Ramella & Suburo, 2015; Yu & Cringle, 2005). The RPE captures photons passing beyond the outer retina, engulfs and degrades oxidized membranous discs, recycles light-absorbing chromophores, produces powerful neuroprotectants and inhibits angiogenesis in the outer retina, securing photoreceptor survival (Thumann, Dou, Wang, & Hinton, 2013).

The first lesions of Age-related macular (AMD), the third global cause of moderate or severe visual impairment (Flaxman et al., 2017), are characteristic extracellular deposits, known as drusen, between the RPE and its basal membrane. AMD reflects the accumulation of oxidative damage induced by phototransduction processes. Imbalance between free radicals and antioxidants impairs RPE functions, slowing

the recycling of downregulating complement factor H (CFH) and up-regulating the vascular endothelial growth factor (VEGF), associated to the neovascular form of AMD (Marazita, Dugour, Marquioni-Ramella, Figueroa, & Suburo, 2016). Oxidative injury is further amplified by genetic and environmental factors (reviewed in: Bellezza, 2018; Datta, Cano, Ebrahimi, Wang, & Handa, 2017; Marquioni-Ramella & Suburo, 2015)).

Yerba mate (YM) leaves (*Ilex paraguariensis*), widely consumed as an infusion (a.k.a. mate) in Argentina, Brasil and Uruguay, have strong antioxidant and anti-inflammatory effects (Bracesco, Sanchez, Contreras, Menini, & Gugliucci, 2011; Heck & De Mejia, 2007). YM improves vascular endothelial function in hyperlipidemic rats (Gao, Liu, Qu, & Zhao, 2013) and lipid profile in healthy and dyslipidemic subjects, reducing the atherogenic effect of high-fat diets (Boaventura et al., 2012; Bravo et al., 2014; de Moraes et al., 2009; Messina et al., 2015). In addition, it has been found useful in obesity (Kim, Oh, Kim, Chae, & Chae, 2015; Pimentel et al., 2013). YM reduces heart infarct size (González Arbeláez et al., 2016), several brain (Bernardi et al., 2019; de Lima et al., 2019) and bone alterations (Brun et al., 2015; Pereira et al., 2017), and can improve cancer-related inflammatory conditions (Cittadini et al., 2019). The phenolic YM fraction, representing 7–10% of its dry weight, explains most YM beneficial effects (Baeza et al., 2014). *Ilex paraguariensis* leaves contain at least 58 polyphenols, mainly (90%) hydroxycinnamic acid derivatives (Mateos, Baeza, Sarriá, & Bravo, 2018). Chlorogenic acids (CHL) are esters of caffeic acid (CAF) and quinic acid (caffeoylquinic acids) and comprise

\* Corresponding author at: IIMT, School of Biomedical Sciences, Universidad Austral, Pilar B1629AHJ, Buenos Aires, Argentina.  
E-mail address: [amsuburo@austral.edu.ar](mailto:amsuburo@austral.edu.ar) (A.M. Suburo).

48% of total YM polyphenols (Mateos et al., 2018; Tajik, Tajik, Mack, & Enck, 2017). CAF content is only 1.7–2.9% of total polyphenols (Becker et al., 2019; Berté, Beux, Spada, Salvador, & Hoffmann-Ribani, 2011). CHL and CAF effects on human health and experimental models have been comprehensively reviewed (de Armas-Ricard, Ruiz-Reyes, & Ramírez-Rodríguez, 2019; Islam et al., 2018).

Polyphenols have been tested on several models of retinal degeneration (Jang et al., 2014; Jang, Choi, Ahn, Jung, & Lee, 2015) and caffeic acid phenethyl ester might reduce RPE oxidative damage (Dinc, Ayaz, & Kurt, 2017; Paeng et al., 2015). Other natural antioxidants, such as resveratrol and quercetin, show similar effects (Sheu, Liu, & Chen, 2013; Sparrow et al., 2003; Wang, Kim, & Sparrow, 2017).

In this work we characterized YM effects on cell death and premature senescence induced by oxidative damage in a cell line derived from human RPE cells (ARPE-19) and we compared these effects with those produced by its main polyphenols, CAF and CHL. In addition, we evaluated polyphenol-induced activation of key molecules implicated in neuroprotection and the endogenous response to oxidative stress (Kamoshita et al., 2016; Lee et al., 2018; Wang et al., 2015; Zhang, Davies, & Forman, 2015): phosphorylation of the cAMP response element binding protein (CREB) (Fu et al., 2017; Matteucci et al., 2014); BCL2, an apoptotic regulator which is under the control of p-CREB (Sugiura et al., 2004); the nuclear factor erythroid 2-related factor 2 (NRF2), superoxide dismutase (SOD2) and sirtuin 1 (SIRT1).

## 2. Materials and methods

### 2.1. Cell culture and experimental substances

The ARPE-19 cells, from the American Type Culture Collection, were cultured in DMEM-F12 (Life Technologies, Invitrogen, Argentina) containing 2.5 mM L-glutamine, 100 U/ml streptomycin/penicillin and 10% fetal calf serum (FCS, NATOCOR, Córdoba, Argentina) at 37 °C and 5% CO<sub>2</sub>.

Hydrogen peroxide (H<sub>2</sub>O<sub>2</sub>) was from Merck Química Argentina (Buenos Aires). YM stock solution (125 mg/ml) was freshly prepared by dissolving instant mate tea (Establecimiento Las Marías, Gdor. Virasoro, Corrientes, Argentina) in hot (80 °C) distilled water, emulating the preparation of mate tea. Further dilutions were in complete medium. Experimental dilutions were 125 and 250 µg/ml (YM125 and YM250). Unless specified, all other chemicals were from Sigma-Aldrich Argentina. Polyphenols, chlorogenic acid (3-(3,4-dihydroxycinnamoyl) quinic acid, CHL) and caffeic acid (3-4-dihydroxycinnamic acid, CAF), were solubilized in ethanol (40 and 112 mM, respectively). Additional dilutions were made in culture medium, and experimental wells contained 100 µM CHL or 70 µM CAF.

Experiments began 1 day after cell seeding, changing the medium in all wells. YM and polyphenol preincubations took place during the first 2 h. After rinsing in 0.01 M phosphate buffered saline, pH 4 (PBS), cells were exposed to H<sub>2</sub>O<sub>2</sub> for 1.5 h. Culture medium was changed and experiments finished as described below. In senescence induction studies, the preincubation and oxidation schedules were repeated for 3 days. Controls remained in medium without additives for the duration of the experiments. However, their culture media were changed together with that of the experimental wells.

### 2.2. Viability assays

ARPE-19 cells were seeded in 96 multiwell plates (10,000 cells/well). The next day they were exposed to 300 or 450 µM H<sub>2</sub>O<sub>2</sub> concentrations (H300 or H450). Viability was evaluated 24 h after exposure to H<sub>2</sub>O<sub>2</sub> by the 3-(4,5-dimethylthiazol-2-yl)-2,5-diphenyltetrazolium (MTT) colorimetric assay (Kumar, Nagarajan, & Uchil, 2018). After medium replacement with a 1:10 dilution of the stock solution (5 mg/ml MTT in PBS), cultures were incubated for 4 hr. The MTT solution was removed and cells were solubilized in 150 µl isopropanol/

0.04 N HCl. Optical densities were measured at 550 nm using the Multiscan FC microplate photometer (Thermo Scientific 1.00.79 MIB 51119000). Three independent experiments were made, with 3–4 wells for each condition (10 wells/experimental point). Results were normalized to controls.

### 2.3. Induction of senescence and senescence-associated β-galactosidase activity

Cells, seeded in 24-multiwell plates (20,000 cells/well), were washed in complete medium and subjected to 150 µM H<sub>2</sub>O<sub>2</sub> during 1.5 hr. Some wells were pre-incubated for 2 h with YM, CAF or CHL, before H<sub>2</sub>O<sub>2</sub> exposure. All treatments were repeated during the first 3 days (indicated as \*3 in graphs). All wells were then cultured in complete medium until day 12th. SA-β-Gal positive and negative cells were identified by histochemical assay. Cells were fixed with 3% formaldehyde in PBS for 5 min and incubated overnight at 37 °C in a staining solution containing 40 mM sodium citrate, pH 6.0, 1% 5-bromo-4-chloro-3-indolyl-β-D-galactopyranoside (X-gal, Promega Corp, Madison, WI), 5 mM potassium ferrocyanide, 5 mM ferricyanide, 150 mM sodium chloride, and 2 mM magnesium chloride (Debacq-Chainiaux, Erusalimsky, Campisi, & Toussaint, 2009). Cultures were examined and scoring was made on 5 photographs from 2 different wells for each experimental point, from 3 to 4 independent experiments. Using this protocol, we found more than 80% of cells showing senescence-associated β-galactosidase (SA-β-GAL) enzymatic activity (Marazita et al., 2016).

### 2.4. Detection of reactive oxygen species (ROS)

ROS intracellular levels were measured with the cell-permeable fluorogenic probe 2',7'-dichlorodihydrofluorescein di-acetate (DCFH-DA) (ThermoFisher, Invitrogen, D399). Cells expanded on 18 × 18 mm coverslips in 6-well plates (30,000 cells/coverslip). After preincubation with polyphenols, a group of wells was subjected to H<sub>2</sub>O<sub>2</sub> oxidation (H150). After transfer to complete medium, all wells received 5 µM DCFH-DA for 30 min. DCFH-DA is deacetylated by cellular esterases. The resulting compound is oxidized by ROS into the fluorescent 2',7'-dichlorofluorescein (DCF). After washing with PBS, photos were taken using a fluorescence microscope (Nikon E800) with a FITC filter. Fluorescence integrated density (pixels/cell) was measured using ImageJ.

### 2.5. Immunohistochemical procedures

For immunofluorescence microscopy, cells were grown on coverslips as described above and PBS rinsed at the end of the experiment. All solutions were made in PBS. Fixation in 4% paraformaldehyde for 20 min, was followed by Triton X-100 (0.1%, 5 min) for permeabilization, and 2% bovine serum albumin (BSA) for blocking. Incubation with primary antibodies (sources and concentrations are described in Table 1) was carried out overnight in 2% BSA. The secondary antibody was Alexa Fluor®488 goat anti-rabbit IgG (Molecular Probes; Invitrogen; dilution 1:500) for 2 hr in blocking solution. After incubation in 2 µg/ml 4',6-diamidino-2-phenylindole (DAPI) for 5 min for DNA detection, coverslips were mounted in PBS-glycerol 1:1. For quantification of immunofluorescent p-H2AX foci, nuclei with ≥5 foci were scored in 50 cells from 2 coverslips per treatment, from 3 experiments.

For Western blots, ARPE-19 cells were seeded in 10 cm plastic dishes (12,000 cells/cm<sup>2</sup>). Cells were harvested in PBS and lysed with 2% sodium dodecyl sulphate (SDS) with 1 mM sodium orthovanadate. Protein concentration was measured with Bradford reagent and adjusted to 22 µg protein/100 µl lysate. 20 µl aliquots were resolved in 15% polyacrylamide gels and analyzed by immunoblotting against p21, p16, p-H2AX, p-CREB, BCL2 (Table 1). Anti-mouse and anti-rabbit secondary antibodies conjugated with horseradish peroxidase (Sigma-

**Table 1**  
Antibodies used in these experiments.

Antigen Abbreviation	From	Source/dilution
p21	Clone SX118, Mouse	BD Biosciences (556430)/1:200
p16 <sup>INK4</sup>	Clone G175-405, Mouse	BD Biosciences (551153)/1:200
γ-H2AX	Rabbit	ABCAM (ab2896)/1:1000
BCL2	Mouse	Santa Cruz (sc-7382)/1:1000
p-CREB	Rabbit	Cell Signaling (87G3)/1:1000
actin	Rabbit (N-terminal antibody)	Sigma-Aldrich (A2103)/1:1000

Aldrich, St. Louis, MO; dilution 1:1000) were used. Signals were enhanced with chemiluminescence detection solution (Solution A: 100 mM Tris pH8.5, 2.5 mM Luminol, 0.4 mM p-Coumaric acid; Solution B: 100 mM Tris pH 8.5, 0.02% H<sub>2</sub>O<sub>2</sub>), and visualized by exposure to light sensitive films (Amersham Hyperfilm TM ECL) or scanned with a LI-COR C-DiGit (Lincoln, NE).

### 2.6. RNA isolation and Quantitative PCR (qPCR)

The General RNA Extraction kit (Dongsheng Biotech, Guangdong, China) was used to isolate total RNA from 10 cm plastic dishes seeded with 12,000 cells/cm<sup>2</sup>. RNA concentration was determined spectrophotometrically (GeneQuant1300 Spectrophotometer). First-strand cDNA was synthesized from 1 μg of total RNA using Superscript II Reverse Transcriptase (Invitrogen, Carlsbad, CA, USA) according to the manufacturer's instructions. Primers for human mRNAs (Table 2) were designed with Primer Blast and synthesized by ThermoFisher (Invitrogen, Argentina).

The relative quantification method (ΔΔCt method) was used to assess mRNA expression levels (Stratagene Mx 3005P System cycler). Each reaction mix (25 μl) contained Power SYBR Green PCR Master Mix (Thermo Fisher) and the specific primers (Table 2). Cycling parameters were 10 min at 95 °C, then 30 sec at 95 °C, 35 sec at 56 °C and 60 sec at 60 °C, for 40 cycles. Expression was normalized to GAPDH. Each reaction was run in triplicate, using dissociation curves to verify the amplification of a single product. Relative amounts of PCR products from untreated cells were set to 1. Each assay included a non-template control.

### 2.7. Statistics

Quantitative data are presented as bar graphs displaying average ± SEM. The number of independent experiments is indicated between brackets in figure captions. For each procedure, we verified normality of numeric results using the Shapiro-Wilks test. Data with a normal distribution were compared using one-way ANOVA, followed by the Holm-Sidak method of pairwise multiple comparisons. The same method, but does not require a previous ANOVA analysis, was performed for non-parametric distributions. Calculations were made with SigmaPlot version 14 (Systat Software, Inc., San Jose California USA, [www.systatsoftware.com](http://www.systatsoftware.com)). Statistical significance is shown as \*, p < 0.05; \*\*, p < 0.01; \*\*\*, p < 0.001.

## 3. Results

### 3.1. Effects of yerba mate extracts on cell survival and senescence

To test YM pro-survival effects, we preincubated ARPE-19 cells with YM125 or YM250 for 2 hr. Control cultures (no YM – no H<sub>2</sub>O<sub>2</sub>) showed the same MTT values as YM-no H<sub>2</sub>O<sub>2</sub> cultures. H300 or H450 reduced viability to 64 ± 2.3% and 56 ± 3.4% of controls (100%). By contrast, in YM125-pretreated cultures, survival reached 86 ± 2% after H300, and 67 ± 7% after H450. YM250 afforded greater protection than YM125, with MTT values attaining 90 ± 3% after YM125 and 85 ± 4% after YM250 (Fig. 1A).

Chronic oxidative stress promotes the onset of the premature cell senescence program both in vitro and in vivo (Fridlyanskaya, Alekseenko, & Nikolsky, 2015). A similar condition was reproduced by low H<sub>2</sub>O<sub>2</sub> concentrations (150 μM) for 1.5 h in 3 consecutive days (H150\*3). These cultures developed premature cell senescence, as shown by over 75% SA-β-GAL + cells after completing 12 days in vitro. YM (YM125\*3 and YM250\*3) preincubation before each H<sub>2</sub>O<sub>2</sub> exposure reduced senescent cells to < 50% (Fig. 1B and C).

Under our experimental conditions, YM in the culture medium did not affect ARPE-19 viability. On the contrary, YM preincubation increased cell survival and prevented premature cell senescence in cultures exposed to oxidative stress.

### 3.2. Effects of CAF and CHL on oxidative stress damage

Polyphenol content might explain YM protection against oxidative stress. Therefore, we tested 70 μM CAF and 100 μM CHL on ARPE-19 survival and senescence activation. These concentrations lie within the range reported by others (Jang et al., 2015; Jeon et al., 2015) and showed no evidence of toxicity in our preliminary experiments-H<sub>2</sub>O<sub>2</sub> exposure reduced viability as in the YM experiments, to 62 ± 2% after H300 and 50 ± 3% after H450. After CAF preincubation for 2 h, MTT values were 90 ± 3% of control values when exposed to H300, and 76 ± 3 when H450 was used. The same pattern appeared in CHL preincubated cultures, which reached 81 ± 9% of control values after H300 and 60 ± 4% in H450 exposed cells (Fig. 2A).

Under senescence promoting conditions, CAF or CHL preincubation reduced the proportion of SA-β-GAL+ cells from 88% to 47% and 45%, respectively (Fig. 2B and C). The increased expression of the cyclin-dependent kinase inhibitors (CKIs) p16 and p21 further verified the senescent state. In line with SA-β-GAL observations, CAF and CHL preincubation decreased these CKIs to 30–47% of untreated exposed cultures levels (Fig. 2D and E). Thus, CAF and CHL reproduced the protecting effects of YM extracts, promoting ARPE-19 cell survival and

**Table 2**  
Forward and reverse Primers used in QPCR.

mRNA	Forward	Reverse
Human NRF2	5' TCTGCCAACTACTCCCAGGT 3'	5' GGGAAATGCTCTGCGCCAAAAG 3'
Human SOD2	GAACCCAAAGGGGAGTTGCT	AGCCTTGGACACCAACAGAT
Human SIRT1	TTCAGTGGCTGGAACAGTGA	ACTGATTACCATCAAGCCGCC
Human GAPDH	5' GGGGCTGCCAGAACATCAT 3'	5' GCCTGCTTCACCACCTTCTTG 3'

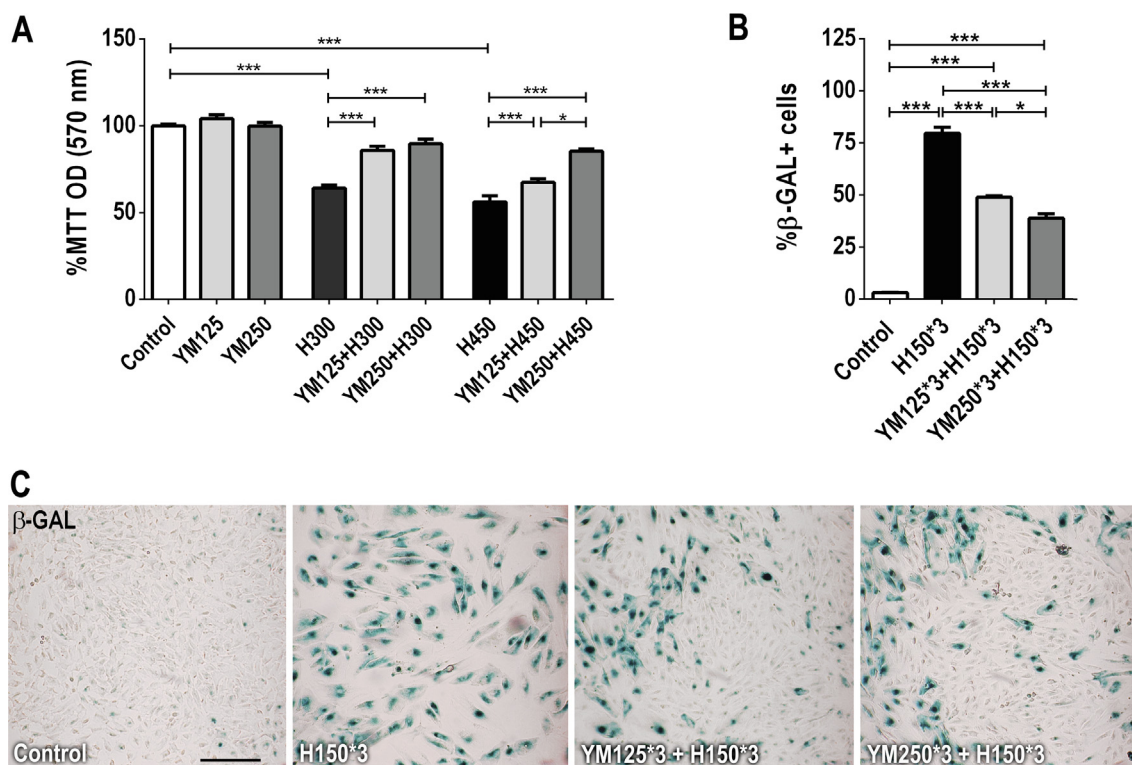


**Fig. 1.** YM protection against oxidative stress. **A.** MTT values, representing cell viability were not changed by YM125 and YM250 preincubation. Exposure to H300 or H450 reduced MTT values, which were partially recovered in cells preincubated with YM ( $n = 10$ ). One-way ANOVA  $p < 0.001$ . In this and all other bar graphs, differences between groups were calculated with the Holm-Sidak method and are indicated by asterisks (\*,  $p < 0.05$ ; \*\*,  $p < 0.01$ ; \*\*\*,  $p < 0.001$ ; \*\*\*\*,  $p < 0.0001$ ). **B.** SA-β-GAL + cells in 12-day ARPE-19 cultures. Oxidative stress increased the proportion of SA-β-GAL + cells, but both YM treatments significantly reduced senescence development ( $n = 3$ ). One-way ANOVA  $p < 0.001$ . **C.** Micrographs show SA-β-GAL + cells. Almost no staining appeared in control cultures, but most cells showed strong staining in  $H_2O_2$  exposed-untreated wells. In YM-treated cultures, only some regions contained the characteristically large SA-β-GAL + cells ( $n = 3$ ).

avoiding senescence.

### 3.3. CAF and CHL reduced markers of oxidative stress and cell damage

To test CAF and CHL effects on cell damage responses, ARPE-19 cultures were subjected to a single 1.5 h H150 exposure. Cells were then incubated with DCFH-DA and observed 30 min later under fluorescence microscopy for ROS detection. No signal appeared in control cultures, but most cells showed intense fluorescence after H150 ( $1.7 \pm 0.3$  px/cell). In polyphenol preincubated wells, fluorescence declined to  $0.6 \pm 0.1$  px/cell and  $0.7 \pm 0.2$  px/cell for CAF and CHL (Fig. 3A and B), implying these polyphenols reduced ROS production.

Since DNA damage is one of the main consequences of oxidative stress, we studied p-H2AX, a phosphorylated histone appearing at DNA breaks sites (Kuo & Yang, 2008). Control wells showed no p-H2AX immunofluorescence, but  $66.0 \pm 0.6\%$  nuclei displayed  $\geq 5$ p-H2AX foci after H150. Preincubation with CAF or CHL significantly reduced these numbers (CAF,  $32.8 \pm 6.3\%$ ; CHL  $41.3 \pm 1.6\%$ ; Fig. 3C and D). In line with immunofluorescence results, control cultures did not show p-H2AX protein, but high amounts appeared in H150 wells tested at 4 and 24 h after the oxidative injury. In CAF + H150 and CHL + H150 cultures, at 4 h, p-H2AX protein was 50% lower than in H150 dishes. At 24 hr, CAF + H150 and CHL + H150 cultures showed the same p-H2AX protein amounts as cells not exposed to oxidative stress (Fig. 3E and F). These results imply that CAF and CHL not only avoided ROS accumulation, but also prevented DNA damage.

### 3.4. Polyphenols activate neuroprotection and antioxidant pathways

The transcription factor p-CREB (Fu et al., 2017) and BCL2, a main

output of the CREB signaling pathway (Wilson, Mochon, & Boxer, 1996), play major roles in neuroprotection and cell survival. In cells not exposed to  $H_2O_2$ , Western blots indicated that CAF or CHL significantly raised p-CREB at the end of the preincubation period (2 h). Without further polyphenol stimulation, p-CREB levels were even higher at 4 h (Fig. 4A and B).  $H_2O_2$  exposure increased p-CREB up to values not different from those induced by polyphenols alone. CAF + H150 and CHL + H150 samples exhibited higher p-CREB levels than polyphenol- or H150 only samples.

BCL2 followed a similar pattern. CAF induced a significant BCL2 increase at the end of preincubation (2 h), which was even higher 2 h later (at 4 h). BCL2 also increased after H150 exposure, achieving similar levels to those induced by polyphenols. In CAF + H150 and CHL + H150 cultures, BCL2 levels almost duplicated those found in ARPE-19 cells receiving either polyphenols or H150 (Fig. 4C and D).

The major antioxidant mechanisms depend on NRF2, SIRT1 and SOD2 (Kamoshita et al., 2016; Mimura, Kaji, Noma, Funatsu, & Okamoto, 2013; Zhang et al., 2015). Therefore, expression of these genes was studied after a 2 h CAF or CHL treatment. At this time, ARPE-19 cells expressed twice the amount of NRF2 and SIRT1 as control cultures. To investigate persistence of this response, we measured the same mRNAs at 4 h, 2 h after polyphenol withdrawal. At 4 h, increases only remained in CAF stimulated cultures (Fig. 5A and B). Both polyphenols significantly upregulated SOD2 expression at 2 h. Increase of SOD2 levels lasted for at least another 2 h without further treatment (Fig. 5C).

## 4. Discussion

In this study we demonstrated that YM and its main polyphenols,

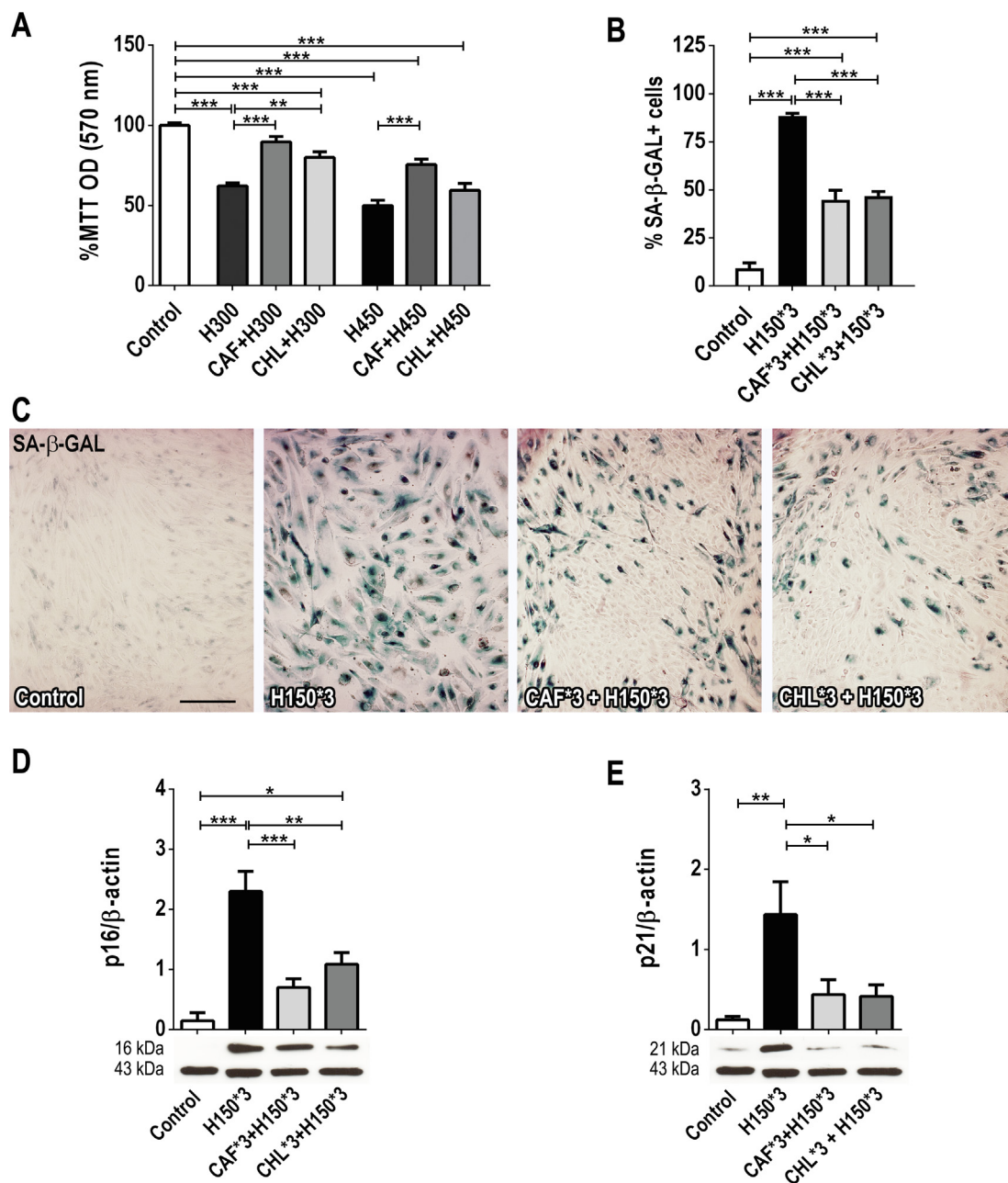


**Fig. 2.** Polyphenol protection against oxidative stress. **A.** H300 or H450 significantly reduced ARPE-19 viability, but CAF and CHL preincubation increased MTT values close to control levels (n = 6). Only Holm-Sidak results are reported. **B.** Bars illustrate the proportion of SA-β-GAL + cells in 12-day ARPE-19 cultures: H<sub>2</sub>O<sub>2</sub> induced SA-β-GAL in 80% of cells, but CAF and CHL preincubation reduced this proportion, indicating a smaller senescent population (n = 4). One-way ANOVA, p < 0.001. **C.** Micrographs illustrating the effects of oxidative stress with and without polyphenol incubation in the proportion of SA-β-GAL + cells. After polyphenol treatment, patches of stained and unstained cells were randomly found within the monolayer (n = 4). Calibration bar, 200 μm. **D and E.** Expression of the CKIs, p16 and p21, detected by Western blotting. In CAF or CHL preincubated samples, damage CKI levels decreased to near control values. Representative blots are shown, indicating the molecular weight of the CKIs in the upper row, and β-actin in the lower row (n = 3). One-way ANOVA, p < 0.001.

CAF and CHL promoted survival and prevented premature senescence in ARPE-19 cells subjected to oxidative stress, an in vitro model of AMD. This model reproduces the hallmarks of this disease, where the role of oxidative stress has been recognized for a long time, both in clinical and experimental studies (Beatty, Koh, Phil, Henson, & Boulton, 2000; Bellezza, 2018; Datta et al., 2017; Hollyfield et al., 2008; Jarrett & Boulton, 2012; Liang & Godley, 2003). Moreover, AMD has been associated with smoking (Myers et al., 2014), which increases exposure to ROS and depletes antioxidants (Suzuki et al., 2008).

#### 4.1. Comparison of protecting effects from YM and its polyphenols

At the chosen concentrations, YM and its polyphenols afforded similar protection. Preincubation with YM125 or YM250 prevented oxidative stress-induced cellular death and premature senescence. Results of similar magnitude were found in cell cultures preincubated with 70 μM CAF or 100 μM CHL. The polyphenol content of YM spray dried preparations, like the product used in our experiments, has been described. An early study showed the presence of 178.32 mg/g of total polyphenols, 91.40 ± 1.75 mg/g CHL and 1.54 ± 0.11 mg/g CAF (Berté et al., 2011). A more recent report yielded comparable results: 123.52 ± 7.87 mg/g CHL, 27.75 ± 1.61 mg/g dicafeoylquinic acid

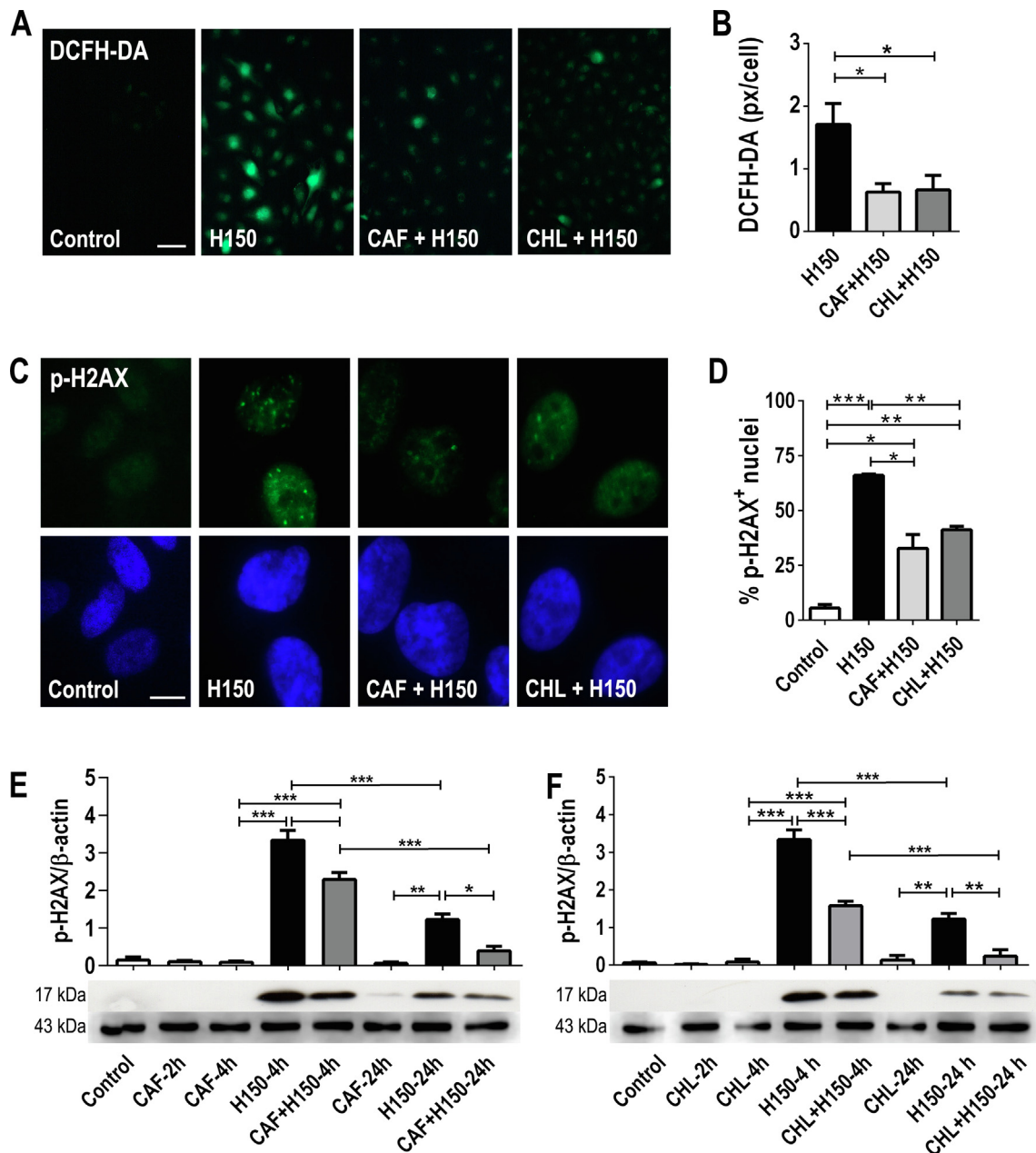


**Fig. 3.** Effects of CAF and CHL on ROS levels and oxidative stress-induced damage. **A.** ROS detection with a fluorescent probe. No signal was found in control cultures, but strong a DCF fluorescence appeared after H150. Little fluorescence appeared in CAF or CHL preincubated cells ( $n = 4$ ). Calibration bar, 100  $\mu\text{m}$ . **B.** Bars representing ROS (DCF) fluorescence (pixels/cell) illustrate the large reduction of cellular ROS when cultures were incubated with CAF or CHL before exposure to oxidative stress ( $n = 4$ ). One-way ANOVA,  $p = 0.022$ . **C.** p-H2AX immunoreactivity (upper row) and DAPI nuclear staining (lower row). Only H150 exposed cultures showed nuclei with several p-H2AX foci. Much less immunoreactivity appeared in polyphenol treated cultures ( $n = 150$ ). Calibration bar, 10  $\mu\text{m}$ . **D.** Proportion of cell nuclei with  $\geq 5$  p-H2AX foci. Results show that most cells were damaged after  $\text{H}_2\text{O}_2$ , but CAF and CHL pretreatment significantly decreased these scores ( $n = 150$ ). One-way ANOVA,  $p < 0.001$ . **E and F.** p-H2AX expression detected by Western blotting (CAF,  $n = 5$ ; CHL,  $n = 4$ ). At 4 h, p-H2AX was very high in H150 exposed cultures but significantly decreased in CAF or CHL pretreated cells. Levels of this damage marker decreased after 24 h. At this stage, p-H2AX values in CAF or CHL pretreated cultures were not different from control values. Images correspond to representative blots, with p-H2AX (MW 17 kDa) in the upper row, and  $\beta$ -actin (MW 43 kDa) in the lower row. Only differences between groups (Holm-Sidak method) are shown.

and  $2.41 \pm 0.22$  mg/g CAF (Becker et al., 2019). Using an average of these results, we estimated that YM250 wells contained 87  $\mu\text{M}$  CHL and 2,7  $\mu\text{M}$  CAF. Since pro-survival and anti-oxidation results after YM250 were in the same range as those supported by 70  $\mu\text{M}$  CAF and 100  $\mu\text{M}$  CHL, the CHL content possibly explains YM protection in vitro.

However, after oral ingestion, gut metabolism will make both polyphenols equally available to cells in vivo (De Oliveira, Sampaio, Pinto, Catharino, & Bastos, 2017; De Oliveira et al., 2017). Caffeic acid is mainly absorbed in the stomach, where little CHL is taken

(Vitaglione, Fogliano, & Pellegrini, 2012). CHL metabolism begins in the stomach and continues in the gut where it is extensively transformed by the colon microbiota to free caffeic or ferulic acids. After YM is given by gavage, rat plasma and liver contain about the same amounts of CHL and CAF (De Oliveira et al., 2017) showing that tissues receive similar quantities of both polyphenols. Other microbial metabolites, such as dihydrocaffeic and dihydroferulic acid, seem to be as effective as CHL in cell protection against oxidative stress (Baeza, Sarriá, Mateos, & Bravo, 2016). Dicafeoylquinic acids could also be

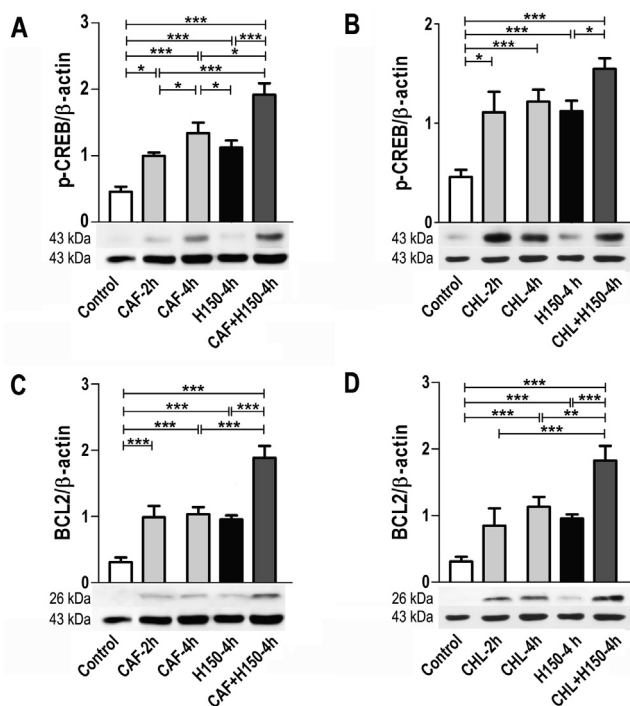


**Fig. 4.** Western blots showing upregulation of p-CREB and BCL2 by oxidative stress and polyphenols. **A** and **B.** CAF and CHL preincubation (2 h) significantly increased p-CREB levels. These high levels remained at 4 h without further polyphenol stimulation. H150-induced p-CREB was not different from that activated by polyphenols. The largest p-CREB levels appeared after CAF + H150 or CHL + H150 (n = 5). One-way ANOVAs, p < 0.001. Representative blots show p-CREB (MW 43 kDa) in the upper row and β-actin (MW 43 kDa) in the lower row. **C** and **D.** CAF significantly increased BCL2 protein at 2 h and both polyphenols were effective at 4 h without further stimulation. BCL2 also increased after H150. The largest rises occurred after polyphenol preincubation and H<sub>2</sub>O<sub>2</sub> exposure (n = 5). Typical blots displaying BCL2 bands in the upper row (MW 26 kDa) and β-actin in the lower row (MW 43 kDa). One-way ANOVAs, p < 0.001.

involved, since they are abundantly found in YM extracts (Becker et al., 2019) and have a greater capacity for ROS scavenging and for NRF2 upregulation than caffeoylquinic acids (Liang, Dupuis, Yada, & Kitts, 2019).

Effective extract and polyphenol concentrations in our *in vitro* model would be compatible with typical human consumption. Average daily ingestion of mate tea (4 cups or 1 l) contains 3.2 g of the spray dried preparation, corresponding to 300–400 mg CHL and 5–8 mg CAF. However, higher polyphenol amounts can be obtained from traditional preparation by hot or cold extraction from YM leaves (Colpo et al.,

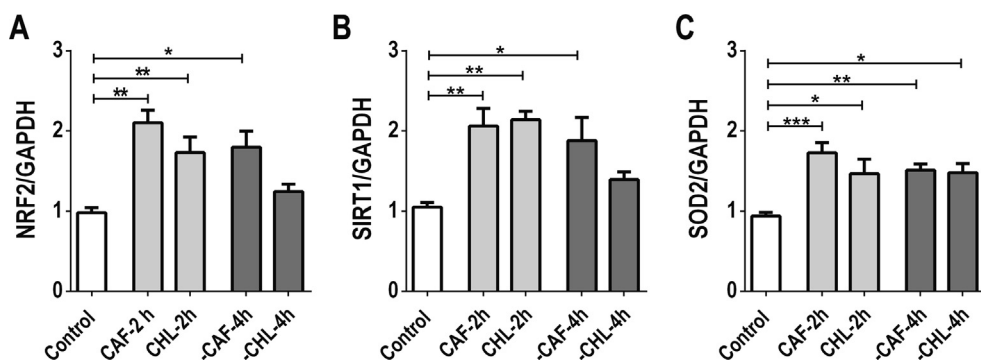


**Fig. 5.** qPCR experiments showing antioxidant gene expression in control and polyphenol-stimulated cultures. Cells were incubated with CAF or CHL for 2 h and remained in polyphenol-free medium for the next 2 h (–CAF 4 h and –CHL 4 h). **A.** NRF2 expression significantly increased after 2 h CAF or CHL incubation. At 4 h, a significant NRF2 increase only remained in CAF stimulated cultures (n = 4). One-way ANOVA, p < 0.001. **B.** SIRT1 expression showed the same activation pattern. Significant increases were observed after polyphenol incubation, but at 4 h, SIRT1 only remained elevated in CAF pre-treated cultures (n = 4). One-way ANOVA, p = 0.002. **C.** CAF and CHL stimulation significantly increased SOD2 expression. High SOD2 levels were still found at 4 h (n = 4). One-way ANOVA, p = 0.001.

2016; da Silveira et al., 2017; Gebara et al., 2017).

#### 4.2. Mechanisms of polyphenol protection in RPE oxidative stress

Fluorescent detection showed that CAF and CHL decreased ROS intracellular accumulation, thus explaining prevention of DNA damage, cell death and senescence induction, together with downregulation of the CKIs p16 and p21. The relative scavenging rate constants for CHL and CAF are much higher than those for Trolox or N-acetylcysteine (Sueishi et al., 2014), suggesting these polyphenols can provide fast control of oxidative environments. YM extracts also show ROS scavenging activity (Colpo et al., 2016; Mateos et al., 2018). However, indirect mechanisms, such as the upregulation of CREB and NRF2, are the main defenders against oxidative stress (Christensen & Christensen, 2014). Both signaling pathways were activated by CHL and CAF.

CREB signaling is one of the most important pro-survival cellular mechanisms (Marinho, Real, Cyrne, Soares, & Antunes, 2014; Pregi, Belluscio, Bernardino, Castillo, & Cánepa, 2017). In addition, CREB upregulates the antioxidant response (Pregi et al., 2017). Artemisinin, a sesquiterpene lactone promoting RPE cell survival, also activates CREB phosphorylation (Chong & Zheng, 2016). In ARPE-19 cultures, CAF or CHL incubation rapidly increased p-CREB, even in the absence of oxidative stress. This transcriptional coactivator remained above control levels for at least two hr after CAF or CHL withdrawal. Moreover, cells subjected to H<sub>2</sub>O<sub>2</sub> after polyphenol preincubation displayed larger amounts of p-CREB than those damaged without previous polyphenol protection. Signaling by p-CREB is involved in the nuclear expression of the DNA repair histone p-H2AX and the upregulation of BCL2, as has been shown in different damage models (Barcia et al., 2015; O’Driscoll, Wallace, & Cotter, 2007; Ye, Shi, Xu, & Huang, 2019).

Under redox balance conditions, NRF2 is bound to Kelch-like ECH-associated protein 1 (Keap1) and rapidly degraded. Polyphenols modify Keap1, inducing NRF2 release and nuclear translocation (Christensen & Christensen, 2014). NRF2 seems to be directly involved in AMD pathogenesis, since *Nrf2*<sup>-/-</sup> mice develop a progressive retinal degeneration including drusen-like deposits, the characteristic lesion of human AMD (Vu & Hulleman, 2017; Zhao et al., 2011). NRF2-dependent mechanisms reduce ROS intracellular levels through the regulation of endogenous antioxidants, phase II detoxification enzymes, and other cellular defensive enzymes, such as SODs, catalase and those involved in glutathione metabolism (Bellezza, 2018). However, ROS optimal levels have yet to be defined. In striated muscle, ROS accumulation is a main cause of sarcopenia. However, the muscle trophic response to exercise requires a certain amount of ROS production and antioxidant supplements can counteract physical exercise benefits (Bellezza, Giambanco, Minelli, & Donato, 2018). On the other hand, natural polyphenols can interact with a large range of cell proteins (Lacroix et al., 2018), suggesting that many other signaling pathways could be involved in their effects.

Comparison of CAF and CHL effects in vitro indicate that, at a lower concentration, CAF produced the same or stronger effects than CHL. Thus, NRF2 and SIRT1 expression remained elevated for 2 h after CAF withdrawal, while these transcripts returned to control levels after CHL withdrawal. SIRT1 expression is reduced in aging retina (Zeng & Yang, 2015) and is dysregulated by oxidative stress (L. Li et al., 2015). It is required for CHL antiapoptotic effects on paraquat-exposed cells (Kong et al., 2019) and can be upregulated by chronic administration of resveratrol (Zeng & Yang, 2015).

SIRT1 and NRF2 upregulation could also be mediated by CREB and both pathways would promote the upregulation of other antioxidant genes like SOD2 (Ding et al., 2016; J. Li et al., 2015; Xia et al., 2017). CAF and CHL also upregulated SOD2, a major defense against superoxide anion and peroxynitrite (Fukai & Ushio-Fukai, 2011).

#### 4.3. The potential role of YM as a functional food

Within the limitations of in vitro experiments, our results suggest that YM, CAF and CHL could protect RPE from degenerative retinal diseases. The decrease of intracellular ROS levels, the activation of antioxidant and pro-survival processes, together with a blockade of premature cell senescence, suggest that YM and these polyphenols could have a role in AMD development and progression. In addition to the pathogenic mechanisms explored here, it has been shown that TGF- $\beta$ 2 induced VEGF expression is completely abrogated by caffeic acid phenethyl ester (Bian, Elnor, & Elnor, 2007), implying a possible role of YM and its polyphenols on neovascular AMD.

Several beneficial effects of YM on diverse health conditions have been described (reviewed in the introduction) and traditional use suggests that this beverage can be consumed in large amounts (Gebara et al., 2017).

#### 4.4. Summary

Our findings show that YM and its polyphenols CAF and CHL can promote survival and decrease senescence progression of an RPE-derived cell line. These changes reflect a direct action on ROS accumulation and the activation of various molecules involved in antioxidant responses such as p-CREB, NRF2, SIRT1 and SOD2. These results support the hypothesis that YM polyphenols, daily ingested as an infusion (mate tea) or in a preparation containing high polyphenol concentrations, could be useful for the prevention of retinal damage in AMD and other retinal degenerations where oxidative stress is a pathogenic mechanism. Therefore, further efforts are required to understand the impact of YM in on the course of AMD and other ageing related conditions. However, studies in vivo are required to support this hypothesis.

#### Ethics statements file

Our research did not include any human subjects and animal experiments

#### CRedit authorship contribution statement

**Pablo S. Tate:** Conceptualization, Investigation, Writing - original draft. **Mariela C. Marazita:** Conceptualization, Writing - original draft. **Melisa D. Marquioni Ramella:** Validation, Writing - original draft. **Angela Maria Suburo:** Conceptualization, Writing - original draft, Supervision.

#### Conflict of interests

The authors declare no conflict of interests.

#### Acknowledgements

Support for this research was provided by: Research fellowships from the Consejo Nacional de Investigaciones Científicas y Técnicas (CONICET), Universidad Austral (PST and MMR) and Agencia Nacional de Promoción Científica y Tecnológica (ANPCyT); MCM and AMS belong to the Research Career from CONICET; AMS is Full Professor of the School of Biomedical Sciences, Universidad Austral (UA). Research funds were provided by UA: T-80020160300002UA-16, I-80020170100007UA-17, T-80020170200014-17, and ANPCyT: PICT 2013-3200.

#### References

- Baeza, G., Amigo-Benavent, M., Sarriá, B., Goya, L., Mateos, R., & Bravo, L. (2014). Green coffee hydroxycinnamic acids but not caffeine protect human HepG2 cells against oxidative stress. *Food Research International*, 62, 1038–1046. <https://doi.org/10.1016/j.foodres.2014.05.035>.
- Baeza, G., Sarriá, B., Mateos, R., & Bravo, L. (2016). Dihydrocaffeic acid, a major microbial metabolite of chlorogenic acids, shows similar protective effect than a yerba mate phenolic extract against oxidative stress in HepG2 cells. *Food Research International*, 87, 25–33. <https://doi.org/10.1016/j.foodres.2016.06.011>.
- Barcia, J. M., Flores-Bellver, M., Muriach, M., Sancho-Pelluz, J., Lopez-Malo, D., Urdaneta, A. C., ... Romero, F. J. (2015). Matching diabetes and alcoholism: oxidative stress, inflammation, and neurogenesis are commonly involved. *Mediators of Inflammation*, 2015, 624287. <https://doi.org/10.1155/2015/624287>.
- Beatty, S., Koh, H., Phil, M., Henson, D., & Boulton, M. (2000). The role of oxidative stress in the pathogenesis of age-related macular degeneration. *Survey of Ophthalmology*, 45(2) 115–134. S0039625700001405.
- Becker, A. M., Cunha, H. P., Lindenberg, A. C., de Andrade, F., de Carvalho, T., Boaventura, B. C. B., & da Silva, E. L. (2019). Spray-dried yerba mate extract capsules: clinical evaluation and antioxidant potential in healthy individuals. *Plant Foods for Human Nutrition*, 74(4), 495–500. <https://doi.org/10.1007/s11130-019-00764-4>.
- Bellezza, I. (2018). Oxidative stress in age-related macular degeneration: Nrf2 as therapeutic target. *Frontiers in Pharmacology*, 9, 1280. <https://doi.org/10.3389/fphar.2018.01280>.
- Bellezza, I., Giambanco, I., Minelli, A., & Donato, R. (2018). Nrf2-Keap1 signaling in oxidative and reductive stress. *Biochimica et Biophysica Acta – Molecular Cell Research*, 1865(5), 721–733. <https://doi.org/10.1016/j.bbamcr.2018.02.010>.
- Bernardi, A., Ballesteros, P., Schenk, M., Ferrario, M., Gomez, G., Rivero, R., ... Ferrario, J. E. (2019). Yerba mate (*Ilex paraguariensis*) favors survival and growth of dopaminergic neurons in culture. *Movement Disorders*, 34(6), 920–922. <https://doi.org/10.1002/mds.27667>.
- Berté, K. A. S., Beux, M. R., Spada, P. K. W. S., Salvador, M., & Hoffmann-Ribani, R. (2011). Chemical composition and antioxidant activity of yerba-mate (*Ilex paraguariensis* A. St.-Hil., Aquifoliaceae) extract as obtained by spray drying. *Journal of Agricultural and Food Chemistry*, 59, 5523–5527.
- Bian, Z. M., Elnor, S. G., & Elnor, V. M. (2007). Regulation of VEGF mRNA expression and protein secretion by TGF- $\beta$ 2 in human retinal pigment epithelial cells. *Experimental Eye Research*, 84(5), 812–822. <https://doi.org/10.1016/j.exer.2006.12.016>.
- Boaventura, B. C. B., Di Pietro, P. F., Stefanuto, A., Klein, G. A., de Moraes, E. C., de Andrade, F., ... da Silva, E. L. (2012). Association of mate tea (*Ilex paraguariensis*) intake and dietary intervention and effects on oxidative stress biomarkers of dyslipidemic subjects. *Nutrition (Burbank, Los Angeles County, Calif.)*, 28(6), 657–664. <https://doi.org/10.1016/j.nut.2011.10.017>.
- Braccesco, N., Sanchez, A. G., Contreras, V., Menini, T., & Gugliucci, A. (2011). Recent advances on *Ilex paraguariensis* research: minireview. *Journal of Ethnopharmacology*, 136(3), 378–384. <https://doi.org/10.1016/j.jep.2010.06.032>.
- Bravo, L., Mateos, R., Sarriá, B., Baeza, G., Lecumberri, E., Ramos, S., & Goya, L. (2014). Hypocholesterolaemic and antioxidant effects of yerba mate (*Ilex paraguariensis*) in high-cholesterol fed rats. *Fitoterapia*, 92, 219–229. <https://doi.org/10.1016/j.fitote.2013.11.007>.
- Brun, L. R., Brance, M. L., Lombarte, M., Maher, M. C., Di Loreto, V. E., & Rigalli, A. (2015). Effects of yerba mate (*Ilex paraguariensis*) on histomorphometry, biomechanics, and densitometry on bones in the rat. *Calcified Tissue International*, 97(5), 527–534. <https://doi.org/10.1007/s00223-015-0043-0>.
- Chong, C.-M., & Zheng, W. (2016). Artemisinin protects human retinal pigment epithelial cells from hydrogen peroxide-induced oxidative damage through activation of ERK/CREB signaling. *Redox Biology*, 9, 50–56. <https://doi.org/10.1016/j.redox.2016.06.002>.
- Christensen, L. P., & Christensen, K. B. (2014). The role of direct and indirect polyphenolic antioxidants in protection against oxidative stress. In R. R. Watson, V. R. Preedy, & S. Zibadi (Eds.). *Polyphenols in human health and disease. Volumen 1: Polyphenols in chronic diseases and their mechanisms of action* (pp. 289–309). Elsevier, Academic Press. <https://doi.org/10.1016/B978-0-12-398456-2.00023-2>.
- Cittadini, M. C., Repossi, G., Albrecht, C., Di Paola Naranjo, R., Miranda, A. R., de Pascual-Teresa, S., & Soria, E. A. (2019). Effects of bioavailable phenolic compounds from *Ilex paraguariensis* on the brain of mice with lung adenocarcinoma. *Phytotherapy Research*, 33(4), 1142–1149. <https://doi.org/10.1002/ptr.6308>.
- Colpo, A. C., Rosa, H., Lima, M. E., Pazzini, C. E. F., De Camargo, V. B., Bassante, F. E. M.,





- International Journal of Molecular Medicine*, 35(5), 1419–1426. <https://doi.org/10.3892/ijmm.2015.2116>.
- Pereira, C. S., Stringheta-Garcia, C. T., da Silva Xavier, L., Tirapeli, K. G., Pereira, A. A. F., Kayahara, G. I. M., ... Nakamune, A. C. de M. S. (2017). Ilex paraguariensis decreases oxidative stress in bone and mitigates the damage in rats during perimenopause. *Experimental Gerontology*, 98(2016), 148–152. <https://doi.org/10.1016/j.exger.2017.07.006>.
- Pimentel, G. D., Lira, F. S., Rosa, J. C., Caris, A. V., Pinheiro, F., Ribeiro, E. B., ... Oyama, L. M. (2013). Yerba mate extract (Ilex paraguariensis) attenuates both central and peripheral inflammatory effects of diet-induced obesity in rats. *Journal of Nutritional Biochemistry*, 24(5), 809–818. <https://doi.org/10.1016/j.jnutbio.2012.04.016>.
- Pregi, N., Belluscio, L. M., Berardino, B. G., Castillo, D. S., & Cánepa, E. T. (2017). Oxidative stress-induced CREB upregulation promotes DNA damage repair prior to neuronal cell death protection. *Molecular and Cellular Biochemistry*, 425(1–2), 9–24. <https://doi.org/10.1007/s11010-016-2858-z>.
- Provis, J. M., Penfold, P. L., Cornish, E. E., Sandercoe, T. M., & Madigan, M. C. (2005). Anatomy and development of the macula: Specialisation and the vulnerability to macular degeneration. *Clinical & Experimental Optometry*, 88(5), 269–281. <https://doi.org/10.1111/j.1444-0938.2005.tb06711.x>.
- Sheu, S.-J., Liu, N.-C., & Chen, J.-L. (2013). Resveratrol stimulates mitochondrial bioenergetics to protect retinal pigment epithelial cells from oxidative damage. *Investigative Ophthalmology and Visual Science*, 54(9), 6426–6438. <https://doi.org/10.1167/iovs.13-12024>.
- Sparrow, J. R., Vollmer-Snarr, H. R., Zhou, J., Jang, Y. P., Jockusch, S., Itagaki, Y., & Nakanishi, K. (2003). A2E-epoxides damage DNA in retinal pigment epithelial cells. Vitamin E and other antioxidants inhibit A2E-epoxide formation. *Journal of Biological Chemistry*, 278(20), 18207–18213. <https://doi.org/10.1074/jbc.M300457200M300457200> [pii].
- Sueishi, Y., Hori, M., Ishikawa, M., Matsu-ura, K., Kamogawa, E., Honda, Y., ... Ohara, K. (2014). Scavenging rate constants of hydrophilic antioxidants against multiple reactive oxygen species. *Journal of Clinical Biochemistry and Nutrition*, 54(2), 67–74. <https://doi.org/10.3164/jcbs.13-53>.
- Sugiura, S., Kitagawa, K., Omura-Matsuoka, E., Sasaki, T., Tanaka, S., Yagita, Y., ... Hori, M. (2004). CRE-mediated gene transcription in the peri-infarct area after focal cerebral ischemia in mice. *Journal of Neuroscience Research*, 407, 401–407. <https://doi.org/10.1002/jnr.10881>.
- Suzuki, M., Betsuyaku, T., Ito, Y., Nagai, K., Nasuhara, Y., Kaga, K., ... Nishimura, M. (2008). Down-regulated NF-E2-related factor 2 in pulmonary macrophages of aged smokers and patients with chronic obstructive pulmonary disease. *American Journal of Respiratory Cell and Molecular Biology*, 39(6), 673–682. <https://doi.org/10.1165/rcmb.2007-0424OC>.
- Tajik, N., Tajik, M., Mack, I., & Enck, P. (2017). The potential effects of chlorogenic acid, the main phenolic components in coffee, on health: A comprehensive review of the literature. *European Journal of Nutrition*, 56(7), 2215–2244. <https://doi.org/10.1007/s00394-017-1379-1>.
- Thumann, G., Dou, G., Wang, Y., & Hinton, D. R. (2013). Cell Biology of the retinal pigment epithelium. In S. J. Ryan (Ed.), *Retina E-Book* (pp. 401–414). Elsevier Health Sciences.
- Vitaglione, P., Fogliano, V., & Pellegrini, N. (2012). Coffee, colon function and colorectal cancer. *Food & Function*, 3(9), 916. <https://doi.org/10.1039/c2fo30037k>.
- Vu, K. T., & Hulleman, J. D. (2017). An inducible form of Nrf2 confers enhanced protection against acute oxidative stresses in RPE cells. *Experimental Eye Research*, 164, 31–36. <https://doi.org/10.1016/j.exer.2017.08.001>.
- Wang, J., Shanmugam, A., Markand, S., Zorrilla, E., Ganapathy, V., & Smith, S. B. (2015). Sigma 1 receptor regulates the oxidative stress response in primary retinal Muller glial cells via NRF2 signaling and system x, the Na-independent glutamate-cystine exchanger. *Free Radical Biology and Medicine*, 86, 25–36. <https://doi.org/10.1016/j.freeradbiomed.2015.04.009>.
- Wang, Y., Kim, H. J., & Sparrow, J. R. (2017). Quercetin and cyanidin-3-glucoside protect against photooxidation and photodegradation of A2E in retinal pigment epithelial cells. *Experimental Eye Research*, 160, 45–55. <https://doi.org/10.1016/j.exer.2017.04.010>.
- Wilson, B. E., Mochon, E., & Boxer, L. M. (1996). Induction of bcl-2 expression by phosphorylated CREB proteins during B-cell activation and rescue from apoptosis. *Molecular and Cellular Biology*, 16(10), 5546–5556. <https://doi.org/10.1130/b25845.1>.
- Xia, X., Qu, B., Li, Y.-M., Yang, L.-B., Fan, K.-X., Zheng, H., ... Ma, Y. (2017). NFAT5 protects astrocytes against oxygen–glucose–serum deprivation/restoration damage via the SIRT1/Nrf2 pathway. *Journal of Molecular Neuroscience*, 61(1), 96–104. <https://doi.org/10.1007/s12031-016-0849-x>.
- Ye, D., Shi, Y., Xu, Y., & Huang, J. (2019). PACAP attenuates optic nerve crush-induced retinal ganglion cell apoptosis via activation of the CREB-Bcl-2 pathway. *Journal of Molecular Neuroscience*, 68(3), 475–484. <https://doi.org/10.1007/s12031-019-01309-9>.
- Yu, D.-Y. Y., & Cringle, S. J. (2005). Retinal degeneration and local oxygen metabolism. *Experimental Eye Research*, 80(6), 745–751. <https://doi.org/10.1016/j.exer.2005.01.018>.
- Zeng, Y., & Yang, K. (2015). Sirtuin 1 participates in the process of age-related retinal degeneration. *Biochemical and Biophysical Research Communications*, 468(1–2), 167–172. <https://doi.org/10.1016/j.bbrc.2015.10.139>.
- Zhang, H., Davies, K. J. A., & Forman, H. J. (2015). Oxidative stress response and Nrf2 signaling in aging. *Free Radical Biology & Medicine*, 88, 314–336. <https://doi.org/10.1016/j.freeradbiomed.2015.05.036>.
- Zhao, Z., Chen, Y., Wang, J., Sternberg, P., Freeman, M. L., Grossniklaus, H. E., & Cai, J. (2011). Age-related retinopathy in NRF2-deficient mice. *PLoS ONE*, 6(4), <https://doi.org/10.1371/journal.pone.0019456>.